Light-Scattering Studies on the Thermally Induced Crystallization Transition of β-Cyclodextrin

Yannis Georgalis,* Jens Schüler, Patrick Umbach, and Wolfram Saenger

Contribution from the Institut für Kristallographie, Freie Universität Berlin, Takustrasse 6, 14195 Berlin, Germany

Received March 10, 1995[⊗]

Abstract: Employing light scattering, we have examined the thermally induced crystallization transition of β-cyclodextrin in the range between 343.2 and 283.2 K with the critical temperature T_c = 307.3 K. The observed cluster evolution resembles the transition from subcritical to postcritical nucleation. The initial cluster size at 343.2 K is 125 ± 21 nm, and the final cluster size at 283.2 K is 400 ± 72 nm with a size of 236 ± 38 nm at T_c. This information can be exploited by means of a simple two-state model so that tentative estimates of the parameters governing β-cyclodextrin nucleation can be extracted according to the classical nucleation theory. The free energy of crystallization at the barrier is $\Delta G_{n_c} = -126 \pm 26$ kJ/mol, and the critical number of seeding particles involved in the formation of such a crystallite is 5. Static light-scattering measurements indicate that subcritical nuclei are more compact than postcritical nuclei. A pronounced hysteresis detected between cooling and heating cycles was further established by light microscopy and digital image analysis.

Introduction

Cyclodextrins (hereafter abbreviated as CD) are a family of four cyclic oligosacchrides, α, β, γ, and δ, comprising six to nine α(1→4)-linked glucopyranose units, respectively.[1,2] Due to their circular structure, CDs form inclusion complexes in aqueous solutions, which crystallize easily. This property renders CDs an excellent model system to study, through X-ray and neutron diffraction, noncovalent molecular interactions. Furthermore, the inclusion of drug molecules is of wide practical importance in the pharmaceutical industry. CDs have also been used as the building blocks of molecular materials and devices for chemically switching on and off biological activity, in particular by photochemical means. Such functions can suit molecular scale devices.[3] Besides "native" CDs, a variety of derivatives with chemically modified O2H, O3H, and/or O6H hydroxyl groups are available.

CDs crystallize readily as "empty" hydrates or inclusion complexes if hot, supersaturated, aqueous solutions of CD with or without added guest molecules are enclosed in a Dewar flask and cooled down slowly. In the crystalline state, the packing of the CD molecules depends on the properties of the enclosed guests.[4,5] If crystallized as hydrates or with small molecular guests, CDs are arranged in a "herringbone" pattern where the cavity of one molecule is blocked on both sides by adjacent, symmetry-related CD molecules (cage structure). With aromatic groups, α-CD forms a cage structure in "brick" pattern. With long molecular or ionic guests, CDs pile up like coins in a roll and the "infinite" cages accommodate the guests (channel structure).

Because of the different crystal packing forms, CDs are attractive for examining the crystallization of simple binary or ternary systems. In this work we have studied the properties of hydrated β-CD·11H_2O that is the most insoluble of all CDs. Its crystal structure has been determined by X-ray and neutron diffraction so that molecular packing and intermolecular interactions are known in detail.[6] β-CD is a torus-shaped molecule, with 15.4 Å outer diameter, 6 Å cavity diameter, and 8 Å height. Its volume is 1500 Å^3. One rim of the torus is lined with O2 and O3 hydroxyl groups and the other with O6 groups, *i.e.*, β-CD is hydrophilic at the outside but the cavity contains C-H groups and is of hydrophobic character.

In earlier work cluster formation of CD hydrates and inclusion complexes was investigated by turbidity measurements.[7] In the present contribution we have employed static and dynamic laser light scattering to investigate the cluster formation occurring upon cooling hot supersaturated aqueous solutions of β-CD. To our knowledge the relevant energetic parameters of cluster formation have not yet been reported by other groups.

Since the degree of residual order is unknown, it is not *a priori* clear whether the observed clusters are crystalline nuclei. We will therefore adopt the term "clusters", instead of "nuclei", to avoid confusion. We will provide persuasive, albeit indirect, evidence that these clusters resemble, with a high probability, nuclei.

Light scattering yields information concerning the size and shape of the growing clusters in a nondestructive equilibrium manner. The analysis of the obtained sigmoidal curves provides conclusions that are not easily duplicated by other techniques. We interpret our results in terms of a simple two-state model that allows estimates of the critical nucleus size, the critical number of nuclei, and the Gibbs free energy of nucleation to be determined.

Theory

Nucleation from the Melt. Experimental verification of the formation of submicroscopic particles of a new phase (nucleation) resulting from a supersaturated solution is not easy and, in certain cases, impossible to prove. Classical nucleation

* To whom correspondence should be addressed. Tel: +030-838-4588. Fax: +030-838-6702. e-mail: yannis@chemie.fu-berlin.de.

⊗ Abstract published in *Advance ACS Abstracts,* August 15, 1995.

(1) Frömming, K. H.; Szejtli, J. *Topics in Inclusion Science*; Kluwer Academic Publishers: Boston, MA, 1994.

(2) Fujiwara, T.; Tanaka, N.; Kobayashi, S. *Chem. Lett.* **1990**, 739.

(3) Arad-Yellin, R.; Green, B. S. *Nature* **1994**, *371*, 320.

(4) Saenger, W. In *Inclusion Compounds*; Atwood, J. L., Davies, J. E. D., MacNicol, D. D., Eds.; Academic Press: London, 1984; Vol. 2, p 231.

(5) Saenger, W. *Israel J. Chem.* **1985**, *25*, 43.

(6) Betzel, K.; Saenger, W.; Hingerty, B. E.; Brown, G. M. *J. Am. Chem. Soc.* **1984**, *106*, 7545.

(7) Szejtli, J.; Budai, Zs. *Acta Chim. Acad. Sci. Hung.* **1979**, *99*, 433.

0002-7863/95/1517-9314$09.00/0

theory[8-10] predicts that the free energy of a crystallite containing n molecules, ΔG_n, depends on its surface free energy, A, and its bulk free energy, B:

$$\frac{\Delta G_n}{k_B T} = An^{2/3} - Bn \tag{1}$$

Assuming spherical nuclei, the values of A and B can be expressed as

$$A = (36\pi)^{1/3}\frac{v_s^{2/3}\sigma}{k_B T} \tag{2}$$

and

$$B = \frac{1}{k_B T}\frac{|\Delta G_m|}{N_A} \tag{3}$$

where ΔG_m denotes the Gibbs free energy difference between solid and liquid phases, σ is the surface free energy per unit area of liquid−crystal interface, k_B is Boltzmann's constant and N_A Avogadro's number, and v_s is the volume per particle in the solid phase. $\Delta G_m/N_A$ is equal with the chemical potential difference in the liquid and solid states or generalized "supersaturation", $\Delta\mu$, the driving force of the nucleation process.

ΔG_n depends on the number of the seeding molecules involved in nucleus formation. A nucleus consisting of a small number of monomers, $n < n_c$, is termed subcritical and may easily dissolve; nuclei with $n > n_c$ grow and form crystals. For small values of n, ΔG_n is positive indicating dissolution of the small nuclei. Metastable equilibrium occurs at the maximum for $n = n_c$ and $d\Delta G_n/dn = 0$. Thermodynamically, a homogeneously supersaturated solution is in a metastable state that may exist for a long time. For crystal growth, the critical energy barrier, ΔG_{n_c}, must be lowered, and this is attained by statistical fluctuations of the free enthalpy in discrete regions of the solution. The mature nucleus consisting of a number of monomers, $n > n_c$, is termed postcritical. In a sense nucleation describes the evolution of postcritical ordered clusters (crystallites).

The limiting free energy of crystallization can be estimated given the number of molecules involved in the nuclei formation:

$$n_c = (32\pi/3)\frac{\sigma^3 v_s^2}{|\Delta G_m/N_A|^3} \tag{4}$$

A consequence of this formulation is that the free energy of a crystallite will increase until the crystallite reaches a critical size, R_c, that includes n_c molecules:

$$R_c = 2\frac{\sigma v_s}{|\Delta G_m/N_A|} \tag{5}$$

Since metastable equilibrium holds $d\Delta G_n/dn = 0$, one can estimate the critical energy barrier that has to be surmounted so that crystallization proceeds spontaneously as

$$\Delta G_{n_c} = (16\pi/3)\frac{\sigma^3 v_s^2}{(\Delta G_m/N_A)^2} \tag{6}$$

Finally, the stationary nucleation rate, J^s, can be estimated to be

$$J^s = Cv_s^{2/3}\left(\frac{\sigma}{k_B T}\right)^{1/2}\frac{k_B T}{h}Zm\exp\left(-\frac{\Delta G_a}{k_B T}\right)\exp\left(-\frac{\Delta G_{n_c}}{k_B T}\right) \tag{7}$$

where C is a constant equal with 2,[10,11] h is Planck's constant, m is a constant involving the number of atoms of liquid per unit volume, Z is the Zeldovich factor,[12] and ΔG_a is the activation energy of the process. Therefore, if ΔG_{n_c} and J^s are known, the activation energy of nucleation can be determined.

Nucleation may be either homogeneous or heterogeneous. Homogeneous nucleation occurs spontaneously, in the absence of foreign particulate material. In contrast, heterogeneous nucleation requires foreign nucleation centers. These may have their origin in the melts employed (*i.e.*, dust) or in the container itself (*i.e.*, scratches on the walls, edges, etc.).

The above theory describes successfully homogeneous nucleation from the melt. Inhomogeneous nucleation, the case encountered in the present study, is different. Here the thermodynamic barrier for homogeneous nucleation is reduced by a factor, $f(\theta)$, involving the wetting angle θ:

$$f(\theta) = \frac{[2 + \cos(\theta)][1 - \cos(\theta)]^2}{4} \tag{8}$$

The type of nucleation may vary from immediate (no barrier has to be overcome and complete wetting occurs) to homogeneous (not wetting at all). For wetting angles other than 180°, the nucleation barrier, eq 6, decreases substantially and the nucleation rate is expected to increase by several times.

Obviously, precise size estimates of the critical nuclei are required for estimating the surface free energy, σ, and the energy difference between liquid and solid states, ΔG_m. The volume of the seeding molecule, v_s, can be readily obtained from the crystal structure, if the latter is available. Further, one can derive the apparent aggregation number, n, from size estimates as a function of temperature or a function of time in quenching experiments.

Most frequently these studies are made by optical or electron microscopy. We will demonstrate that light scattering can also provide the required information. One distinct advantage is that one can examine nucleation in a nonperturbing equilibrium manner. The method as such has been reviewed in several monographs and articles.[13-15] Below we will give only a brief description of the technique necessary for the interpretation of the experiments.

Light Scattering. Dynamic Light Scattering (DLS). DLS provides direct means for determining the free-particle diffusion coefficient for dilute suspensions of monodisperse particles. This is true only if the particles do not interact with each other and their hydrodynamic radius, R, is small compared to the employed wavelength ($R < \lambda/20$).

(8) Zettlemoyer, A. C., Ed. *Nucleation*; Marcel Dekker Inc.: New York, 1969.
(9) Oxtoby, D. W. *Adv. Chem. Phys.* **1988**, *70*, 263.
(10) Hurtle, D. T. J., Ed. *Fundamentals of Crystal Growth, Thermodynamics and Kinetics*; North Holland Publishing: Amsterdam, The Netherlands, 1994.
(11) Walton, A. G. In *Nucleation*; Zettlemoyer, A. C., Ed.; Marcel Dekker Inc.: New York, 1969.
(12) Chernov, A. A. *Modern Crystallography III*; Springer-Verlag: Berlin, Germany, 1984.
(13) Schmitz, K. S. *An Introduction to Dynamic Light Scattering by Macromolecules*; Academic Press: New York, 1990.
(14) Brown, W., Ed. *Dynamic Light Scattering, the Method and Some Applications*; Oxford Science Publications: Oxford, U.K., 1993.
(15) Schaefer, D. W.; Bunker, B. C.; Wilcoxon, J. P. *Proc. R. Soc. London A* **1989**, *423*, 35.

The electric field autocorrelation function (ACF), $G^{(1)}(\tau)$, is a quantity that is proportional to the distribution of relaxation times τ and scattering amplitudes of the examined components. The formulation of the field ACF involves an integration over the size distribution function to account for polydispersity and eventual polymodality:

$$G^{(1)}(\tau) \propto \int_{R_{min}}^{R_{max}} N(R)M^2(R)P(\mathbf{q})S(\mathbf{q}) \exp(-mR^{-1}\mathbf{q}^2\tau_{rel})dR \quad (9)$$

where m is a proportionality constant, $N(R)$ and $M(R)$ denote number and mass of particles with radius R in the size range between R_{min} and R_{max}, $P(\mathbf{q})$ and $S(\mathbf{q})$ denote the form and static structure factors, respectively, $\mathbf{q}$ is the scattering vector equal with $(4\pi n/\lambda)\sin(\theta/2)$, n is the refractive index, and θ is the scattering angle. Polymodality and polydispersity can be resolved with adequate precision by Laplace inversion of the ACF. The simple expansion of the decay rates adopted in the present study provides only mean size estimates and approximate measures of the solution polydispersity. Such a scheme is suitable for monomodal−low-polydispersity samples; accounts of the resolution and limitations of several DLS analysis schemes are given elsewhere.[13,14]

Ideally, eq 9 delivers the z-average hydrodynamic radius R that is associated with the free-particle diffusion coefficient, via the Stokes−Einstein equation:

$$D = \frac{k_B T}{6\pi\eta R} \quad (10)$$

where η is the viscosity of the solvent.

Static Light Scattering (SLS). The intensity scattered at a given angle can be expressed as

$$I(\mathbf{q}) \propto \int_{R_{min}}^{R_{max}} N(R)M^2(R)P(\mathbf{q})S(\mathbf{q})dR \quad (11)$$

The static structure factor can be obtained from measurements of the angular dependence of the total scattered light. For monomodal and monodisperse solutions, $N(R)$ can be determined with adequate precision from $I(\mathbf{q})$ if particle size estimates are available. In addition, both $P(\mathbf{q})$ and $S(\mathbf{q})$ can be reliably approximated if the particle size and shape are known.

For spherical scatters, $S(\mathbf{q})$ can be written as

$$S(\mathbf{q}) = 9(\mathbf{q}R_g)^{-6}[\sin(\mathbf{q}R_g) - \mathbf{q}R_g\cos(\mathbf{q}R_g)]^2 \quad (12)$$

where R_g is the radius of gyration of the particle. The expression for the form factor is equivalent; the seed particle radius is used instead of R_g. For spherical scatterers, R_g is associated with the hydrodymamic radius through the simple expression $R_g = \sqrt{3/5}R$.

For scatterers that are large in comparison with the employed wavelength, the intensity scales as a function of the scattering vector $\mathbf{q}$ with a characteristic exponent, p:

$$I(\mathbf{q}) \propto \mathbf{q}^{-p} \quad (13)$$

In general, p is associated with the dimensionality of the particles and may take different values, depending on the spatial resolution and their properties, *i.e.*, if they are smooth spheres or ramified structures. Detailed descriptions of the scaling properties of $I(\mathbf{q})$ have been given by several authors.[15−17]

In the power law region, p can be written as $p = -2d_f + d_s$, and it can be employed for characterizing compactness and smoothness of the examined particles through their characteristic mass, d_f, and surface, d_s, fractal dimensions.

For mass fractals, the surface scales with mass, and it holds $d_f = d_s$ and $p = -d_f$. Surface fractals are uniformly dense so that $d_f = 3$ and $p = -6 + d_s$. Using the slopes, one can identify mass and surface fractals as structures with p greater than and less than -3, respectively, if power law behavior is obeyed. In cases where interfacial layers are present, scattering profiles with $p < -4$ can be often observed.

Materials and Methods

β-CD was purchased from Sigma Chemical Co. (Lot 47F-3509). Since the solubility of β-CD in water at room temperature, is only 19 mg/mL,[18] preweighted quantities of β-CD were dissolved in boiling, degassed triply distilled water and incubated for 10 min at 343.2 K. These precautions are necessary to avoid the formation of microbubbles during cooling of the solutions and for controlling the initial cluster size distribution. Solutions were rapidly filtered through 800 μm pore size filters, and light-scattering measurements were initialized immediately at 343.2 K.

Viscosity corrections at different temperatures were made by interpolation using standard values for water.[19] Since the solute supersaturation is known as a function of temperature,[18] a temperature gradient can easily be transformed to a supersaturation gradient, if necessary.

Data Acquisition and Evaluation. DLS measurements were conducted with an ALV/SP-86 spectrogoniometer (ALV, Langen, Germany) and the ALV-5000/FAST digital autocorrelator boards at a scattering angle of 90°. A tunable Ar^+ laser (488 nm) was employed as light source. The temperature was adjusted by a Lauda RC6 thermostat and a programmable gradient driver (Lauda PM351). The cooling rate was kept constant in all DLS experiments, 0.25 K/min, and the ACF sampling rate was 120 s/spectrum.

The β-CD monomer volume can be directly obtained from the known X-ray structure,[6] $v_0 = 1.5$ nm^3. An equivalent monomer radius, $R_0 = 0.71$ nm, can be computed from the monomer volume. This size is below the detection limits of DLS even when very fast correlation is employed. Theoretically, the monomers are expected to contribute in the ACF spectra only as a time dependent background.

Since the particle distributions were monodisperse and monomodal with a variance less than 10%, the spectra were analyzed with the ALV cumulant expansion of the decay rates.[20] We have used a fourth-degree fitting with form factor weights for spheres. Typical ACFs including the cumulant fits are displayed in Figure 1. They are of a single-exponential form, and their characteristic relaxation times indicate particle growth with decreasing temperature.

The mean particle size estimates at each temperature were assumed to obey sigmoidal kinetics. A simple four-parameter Boltzmann equation can be employed for modeling the data:

$$R(T) = \frac{R_A - R_B}{1 + \exp(m)} + R_B$$

$$\text{with } m = -\frac{\Delta T}{dw} \quad (14)$$

$R(T)$ denotes the particle radius at temperature T, and R_A and R_B are the initial and final cluster radii, respectively. $\Delta T = T_c - T$ denotes the supercooling, T_c is the critical temperature at 50% of the transition, and dw is the half-width at half-height of the peak resulting after differentiating $R(T)$ with respect to T.

At T_c the nucleation rate is expected to be maximum. The mean particle radius at this temperature has thus been termed R_c. Typical

(16) Porod, G. *Kolloid-Z.* **1951**, *124*, 82. Porod, G. *Kolloid-Z.* **1952**, *125*, 51. *Ibid.* 109.

(17) Tchoubar, In Neutron, X-Ray and Light Scattering; Lindner, P., Zemb, Th., Eds.; Elsevier Science Publishers B. V.: Amsterdam, The Netherlands, 1991; p 157.

(18) Szejtli, J. *Cyclodextrins and their Inclusion Complexes*; Akadémiai Kiadó: Budapest, Hungary, 1982.

(19) *The CRC Handbook of Chemistry and Physics*, 65th ed.; The Chemical Rubber Co.: Cleveland OH, 1984−1985.

(20) Koppel, D. E. *J. Chem. Phys.* **1972**, *57*, 4814.

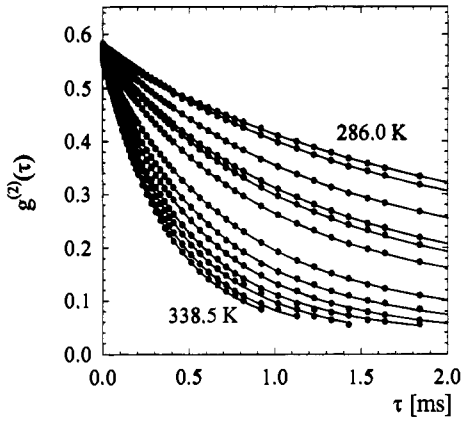

Figure 1. DLS spectra of β-CD (48.9 mg/mL) in water, in the range between 338.5 and 286 K. Spectra were collected at a scattering angle of 90°. For clarity only the initial slope of every tenth spectrum is displayed. The temperature difference between consecutive spectra corresponds to 4 ± 0.1 K. The solid line through the points indicates the fourth-order cumulant fit on the decay rates.

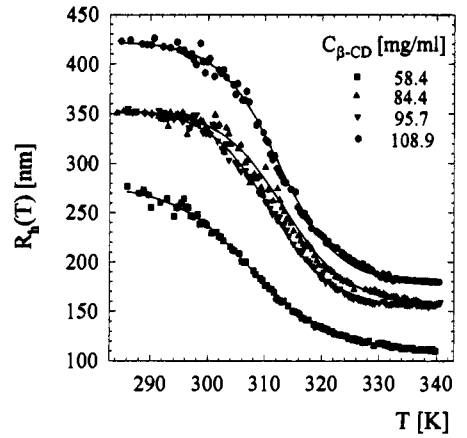

Figure 2. Typical cluster evolution records of β-CD monitored by DLS as a function of temperature. The solid lines indicate the sigmoidal Boltzmann fits, eq 14, and corroborate a two-state model governed by an apparent equilibrium constant, K, eq 17. The parameters determined from the nonlinear Boltzmann fits are given in Table 1. For clarity only every second experiment is shown.

experiments indicating the particle size evolution as a function of temperature during crystallization of β-CD are displayed in Figure 2. The solid line through the data indicates the Boltzmann fit.

Relative estimates of the number of clusters can be obtained if one combines the size and scattered intensities estimates according to eq 11, normalized appropriately with the form and structure factors. Since all these observables are functions of both β-CD concentration and temperature, they can be further recast as illustrative three-dimensional and spectral plots using standard inverse weighting algorithms.[21]

Static Light Scattering. Small-angle SLS experiments were conducted employing an apparatus of similar geometry to that described by Schätzel.[22,23] Scattered light was detected by an 8-bit CCD camera (Sony ICX 039 chip) distributed by Cheops Co. (München, Germany). In its present configuration, the angular range extends from 1.2° to 13.6° and corresponds to a scattering vector range between 2.8×10^{-4} and 3.1×10^{-3} nm^{-1} for the He−Ne laser, wavelength 632.8 nm. Scattered intensities were computed after circular averaging of bitmaps and plotted as ln $I(\mathbf{q})$ vs $\mathbf{q}^2$. The slopes and intercepts obtained from linear least-squares fits can be associated with R_g and $I(0)$, respectively.

Finally, conventional SLS experiments were conducted with the ALV/SP-86 spectrogoniometer. The temperature range between 343.2 and 298.2 K has been examined for β-CD solutions with an intermediate concentration of 60 mg/mL. The angular range exploited was between 20° and 100° with a step of 2.5°. Scattered intensities were plotted as a function of the scattering vector $\mathbf{q}$ in a double-logarithmic manner. Lower temperatures were not explored due to growth of crystallites on the light-scattering walls below room temperature. The data were plotted logarithmically as scattering amplitudes ln $I(\mathbf{q})$ vs wave vector ln $\mathbf{q}$, and the slopes $p(T)$ were determined from linear least-squares fits.

Light Microscopy. Temperature-resolved images of the crystallization process were recorded with an Axiovert 100 inverted microscope (Zeiss, Germany) employing a long distance objective lens (Achrostigm 32X, Zeiss). The overall magnification of the images is 1000× as judged by calibration with standard grids. Experiments were conducted in thermostated quartz slide cells, with a pathlength of 1 mm. Gradients were driven as mentioned above, and a second CCD camera was used for acquiring the images at preselected time intervals. Commercially available and home-written software were employed for the recognition and labeling of the digitized components. This procedure allows a temperature-resolved reconstruction of the distribution of large crystallites which renders additional support to the light-scattering results.

Combination of the equipment described in this section offers the opportunity to investigate cluster growth and crystallite formation within 6 orders of magnitude in space (from nanometer to millimeter range) in a time (temperature)-resolved fashion.

Results and Discussion

Two-State Model. We postulate that close to the critical temperature, T_c, the transition from subcritical to postcritical nucleation takes place. This hypothesis emerges from the appearance of the crystalline phase slightly above T_c, as judged by optical microscopy.

We have at first to make sure that the clusters we are dealing with are the smallest clusters possible at high supersaturation. We also have examined filtered β-CD solutions at concentrations of 3−10 mg/mL which were kept at 343.2 K under transient nucleation conditions. Stable and monodisperse aggregates of 100−150 nm size were found reproducibly in these experiments. We have to mention that β-CD solutions diluted to 0.5 mg/mL, incubated for 1 h at 343.2 K, and ultrasonicated for 30 min contain appreciable amounts of such clusters. Their nominal size under those extreme conditions is not smaller than 80 nm, thus exceeding by 2 orders of magnitude the size of β-CD monomers. An interpretation for the formation of these clusters is difficult and out of the scope of the present work. We have collected a large amount of DLS results on this issue. It will be presented in a subsequent communication together with simple theoretical considerations.

The occurrence of these clusters indicates that the nucleation burst is very rapid, and it may occur already at 343.2 K when β-CD is dissolved in water. Therefore subcritical nuclei are already present at this temperature, but their formation escapes by light-scattering methods. While we can not exclude the possibility that subcritical nucleus formation may obey more complex mechanisms than anticipated by classical considerations, we will focus on the observed subcritical to postcritical nucleus transition.

If the volume changes associated with a phase transition are relatively small, the Gibbs free energy can be used to describe the process. The theory employed for deriving the crystallization parameters considers a simple two-state model involving growth of large from small clusters.

The free energy change, ΔG, associated with the conversion of a subcritical to a large, postcritical cluster is given by

$$\Delta G = \Delta H - T\Delta S \tag{15}$$

Estimates for the free energy can be obtained by setting

(21) Stanford Graphics Presentation and Analysis Package, 3-D Visions, 1994.

(22) Schätzel, K.; Ackerson, B. J. *Phys. Rev. Lett.* **1992**, *68* (3), 337.
(23) Schätzel, K.; Ackerson, B. J. *Phys. Rev. E* **1993**, *48* (5), 3766.

$$\frac{\Delta G}{N_A} = -k_B T \ln K \tag{16}$$

where K denotes an apparent equilibrium constant defined as

$$K = \frac{R_B - R(T)}{R(T) - R_A} \tag{17}$$

We have compiled in Table 1 the values obtained from the sigmoidal fits of eight selected experiments. Since it is difficult to claim systematic tendencies of the data as a function of the initial β-CD concentration, we have averaged the results.

Mean values for the slope of the transition can be determined as $dw = 5.95 \pm 0.63$ nm/K. Similarly the observed critical temperature is determined as $T_c = 307.32 \pm 3.66$ K with an uncertainty of about 10%. The deviations of the mean cluster size at 343.2 K are small, $R_A = 135 \pm 21$ nm. Larger deviations are observed for the cluster size at the transition point, $R_c = 236 \pm 38$ nm, as well as for the terminal size of the cluster at the final temperature of 283.2 K, $R_B = 400 \pm 72$ nm. One should notice that clusters grown at 343.2 K exhibit a size increment of *ca.* 100% at T_c and 300% at the final temperature of 283.2 K. Initially, β-CD clusters with a mean size of 136 nm contain 6.9×10^6 monomers, assuming a spherical shape. At saturation, the cluster size reaches 400 nm and the number of particles involved increases by 26 times to 1.8×10^8.

The larger standard deviations below T_c have their origin in several sources: (1) the appearance of microcrystallites that either sediment and cross through the scattering volume or stick on the walls of the light-scattering cells (see discussion below) and destroy several spectra and (2) difficulties to precisely control the initial distribution of clusters. In either case, size estimates of the clusters are expected to be subject to uncertainties due to the randomly distributed nucleation centers. Therefore, the fluctuations observed in the experiments are not unjustified. However, we will show that the mean sizes determined suffice for a first-order approximation of the Gibbs free energy.

Plots of ln K versus $1/T$ are linear, Figure 3, as judged by the correlation coefficients of linear least-squares fits. ΔG is determined as -126 ± 26 kJ/mol and describes adequately the experimental data. If entropy contributions are assumed to be small, the calculated enthalpies correspond within a factor of 2 or less to the enthalpy determined for silicate glasses[24-26] and resemble closely the enthalpy of formation of purely ionic crystal lattices, $-600-1000$ kJ/mol.[27]

The linear behavior exhibited by the ln K vs $1/T$ plots implies that the reaction enthalpy of cluster formation is only a weak function of temperature. The observed transition is therefore expected to be accompanied by negligible changes of the heat capacity. Calorimetric experiments are theoretically expected to provide a reliable comparison, and van't Hoff analysis should yield similar estimates of ΔH as the DLS experiment. For a first-order crystallization transition (homogeneous nucleation), a singularity of the derivative $(\partial \Delta C_p / \partial T)$ is expected at T_c. It is however doubtful whether this can be observed for nonhomogeneous nucleation. We have conducted a few differential scanning calorimetry (DSC) experiments, under conditions comparable to those of the DLS experiments using a Microcal MC-2 (Microcal Inc.) scanning calorimeter. The cooling cycle was examined between 343.2 and 293.2 K with a rate of 0.16 K/min. ΔC_p was determined to be only 0.097 kcal/mol/K and $T_c = 306.4 \pm 0.5$ K, consistent with that determined by DLS. The effect is rather small, corroborating the above hypothesis.

Table 1. Fitting Parameters Derived from Eq 14 for Data Shown in Figure 4[a]

c_0 (mg/mL)	dw (nm/K)	T_c (K)	R_c (nm)	R_A (nm)	R_B (nm)
49.0	6.7 ± 0.5	303.1 ± 0.9	296 ± 10	114 ± 2	477 ± 21
58.4	5.5 ± 0.5	307.9 ± 0.7	198 ± 13	123 ± 3	285 ± 9
60.6	6.7 ± 0.3	309.8 ± 0.7	306 ± 12	157 ± 3	492 ± 46
71.9	5.4 ± 0.4	310.4 ± 0.4	311 ± 17	160 ± 6	475 ± 6
84.4	6.7 ± 0.6	307.4 ± 0.7	255 ± 10	163 ± 2	349 ± 4
95.7	5.5 ± 0.5	308.1 ± 0.5	253 ± 18	157 ± 3	352 ± 4
108.9	5.2 ± 0.4	312.4 ± 0.4	310 ± 21	188 ± 6	425 ± 15
116.7	5.9 ± 0.9	303.4 ± 0.9	213 ± 17	178 ± 4	349 ± 4
mean	5.9 ± 0.6	307.3 ± 4.0	236 ± 38	135 ± 21	400 ± 72

[a] Eight experiments with β-CD in the concentration range between 49.0 and 116.7 mg/mL are displayed with the average value and standard error of each parameter.

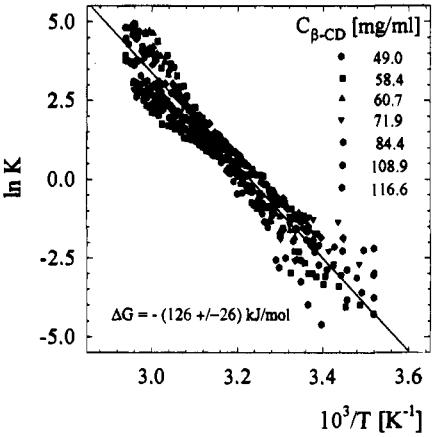

Figure 3. Plot of ln K, defined in eq 17, vs reciprocal temperature, $1/T$. The solid line indicates the best linear least-squares fit. Higher order fits were not justified despite minor deviations in some of the data sets.

Mechanism of Cluster Growth. We can now compare the experimentally derived values with the theoretical predictions. One can differentiate between three types of cluster growth. (1) Simple growth: Addition of a monomer is favorable to about the same degree for all monomers. Aggregation begins when two monomers form a dimer, and then another monomer is added to become a trimer, etc., until the aggregate transforms to a macroscopic phase. A typical example is the diffusion-limited monomer–cluster aggregation (DLA). In this type of aggregation the free energy is negative and approximately equal for all monomers, independent of the cluster size. The free energy is a function of size and drops linearly from zero to large negative values. (2) Exponential growth: Addition of the next monomer is more favorable than that of the preceding unit (positive cooperativity). Large clusters appear to be "stickier" than small ones, similar to growth in the diffusion-limited cluster–cluster (DLCA) aggregation. The free energy starts from zero and relaxes exponentially to large negative values. (3) Nucleation-controlled growth: Formation of large aggregates is preferred in comparison to formation of small ones. The free energy of monomer addition is positive for small aggregates, reaches a maximum that identifies the size of the critical nucleus, and crosses to negative values for larger cluster sizes. In this case structures smaller than critical nuclei will be unstable and in some stage will dissolve.

(24) Rowlands, E. G.; James, P. F. In *The structure of Non-Crystalline Solids*; Gaskell, P. H., Ed.; Taylor and Francis: London, U.K., 1977; p 215.

(25) Kröger, C.; Keitlow, G. *Glastech. Ber.* **1959**, *29*, 393.

(26) Crammer, D.; Salomaa, R.; Yinnon, H.; Uhlamm, D. R. *J. Non-Cryst. Solids* **1981**, *45*, 127.

(27) Atkins, P. W. *Physical Chemistry*; Oxford University Press: Oxford, U.K., 1986.

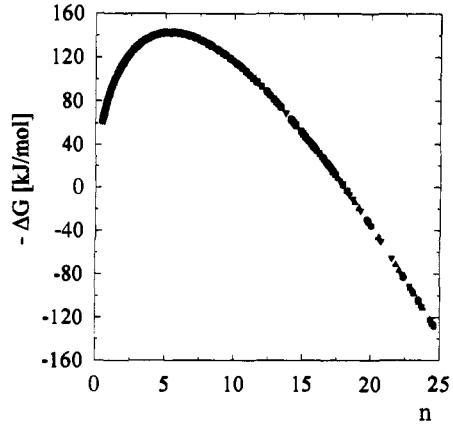

Figure 4. Plot of the approximate free energy, ΔG_n, of the formation of crystallites, eq 1, as a function of the number of seeding molecules, n. For these computations we have employed all data sets shown in Table 1 and calculated the mean values of $A = 3.83 \times 10^6$ and $B = 1.46 \times 10^6$ at the transition. For the interfacial tension we have used 0.071 J/m^2 as determined for β-CD in water by tensiometry.[1] All data sets scale on a single master curve indicating nucleation controlled growth. ΔG_{n_c} and n_c are estimated to be −145 kJ/mol and 5, respectively.

Solving eq 5 with the mean estimates shown in Table 1, we obtain $\Delta G_m = 0.54$ kJ/mol. We can then compute the surface free energy, A, and the bulk free energy, B, from eqs 2 and 3. At the transition we obtain the following mean values: $A = 3.83 \times 10^6$ and $B = 1.46 \times 10^6$. Assuming spherical clusters, we can then estimate the aggregation number of a nucleus at any temperature as the ratio:

$$n = (v_n/v_s) = [R(T)/R_A]^3 \qquad (18)$$

for each data set and plot it as a function of the compound ΔG_n. It can be shown, Figure 4, that all eight data sets collapse on a single master curve with a maximum that corresponds to $n_c = 5$ and $\Delta G_{n_c} = -145$ kJ/mol. This picture corroborates that the cluster growth of β-CD can be identified as nucleation-controlled.[9,28]

Kinetic Nucleation Experiments. Kinetic nucleation experiments were conducted at constant temperatures below and above T_c with solutions at a single intermediate β-CD concentration of 60 mg/mL prepared at 343.2 K. Apparent decay rates of the nucleation reaction were determined through the expression:

$$R(t) = a_0[1 - \exp(-t\tau)] \qquad (19)$$

Selected experiments are displayed in Figure 5. The initial size of these aggregates is in noticeable agreement with the size determined in the temperature gradient experiments, Figure 2. The size of the aggregates nucleating in the proximity of T_c (307.3 K) is considerably larger than those below or above it. The decay rates, τ, corresponding to typical quenches at 313.2, 308.2, 303.2, and 298.2 K are $(8.07 \pm 0.03) \times 10^{-4}$, $(3.86 \pm 0.08) \times 10^{-3}$, $(1.56 \pm 0.04) \times 10^{-3}$, and $(2.27 \pm 0.03) \times 10^{-3}$ s^{-1}, respectively. These values indicate that around T_c the nucleation rate is, as expected, maximum.

Compactness and Surface Roughness of the Clusters. For nucleation and growth, small, uniformly dense, $d_f = 3$, and smooth-surfaced, $d_s = 2$, domains are expected to evolve. The mass of the domains increases, but the surface area, which is proportional to d_s in the power law regime, decreases. Therefore, in the ideal case, $p(T)$ for spherical clusters should be equal or very close to −4.

In Figure 6a we display a typical conventional SLS experiment that involves a temperature variation as described in the Materials and Methods section. When the temperature is lowered, the exponents assume lower values and remain nearly stable below T_c, Figure 6b. This observation is compatible with a roughening of the surface as nucleation progresses. Therefore, at high temperatures one claim compact structures that gradually change to ramified and rough ones during the transition from subcritical to postcritical nucleus formation. The roughening

(28) de Young, L. R.; Fink, A. L.; Dill, K. A. *Acc. Chem. Res.* **1993**, *26*, 614.

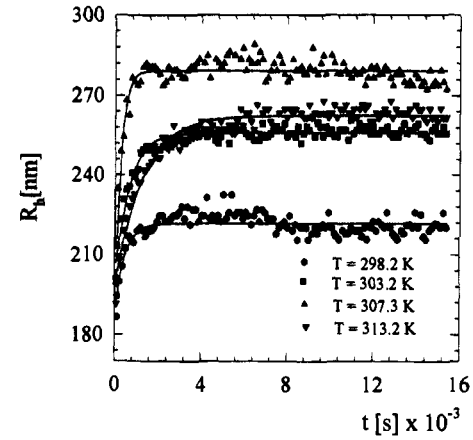

Figure 5. Kinetic nucleation experiments of β-CD at 60 mg/mL. The solid lines denote the nonlinear fit indicated by eq 19. It is noteworthy that during quenching at temperatures below and above T_c, the growth rates are 2−4 times slower than that at T_c.

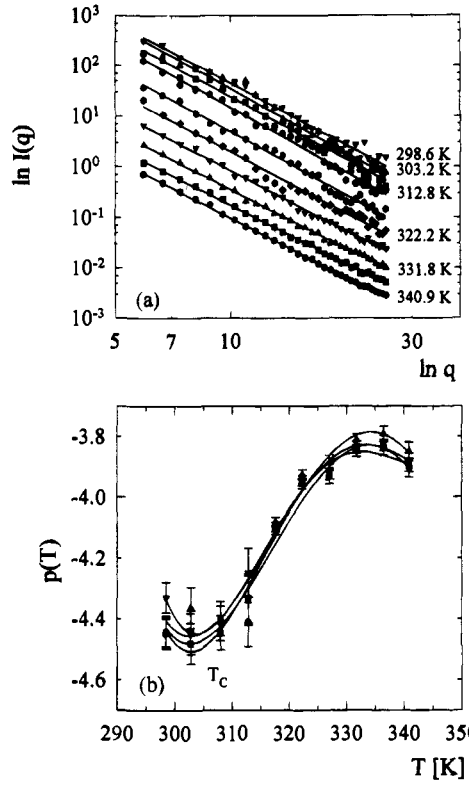

Figure 6. (a) Typical double-logarithmic plots of the total scattered intensity as a function of the scattering vector **q** recorded at different constant temperatures. The angular range exploited was between 20° and 100°. (b) Resulting scaling exponents, $p(T)$, plotted as a function of temperature for four identical experiments. They range between −3.8 and −4.5 indicating that the clusters change from compact to ramified structures, probably surrounded by interfacial layers, while nucleation progresses.

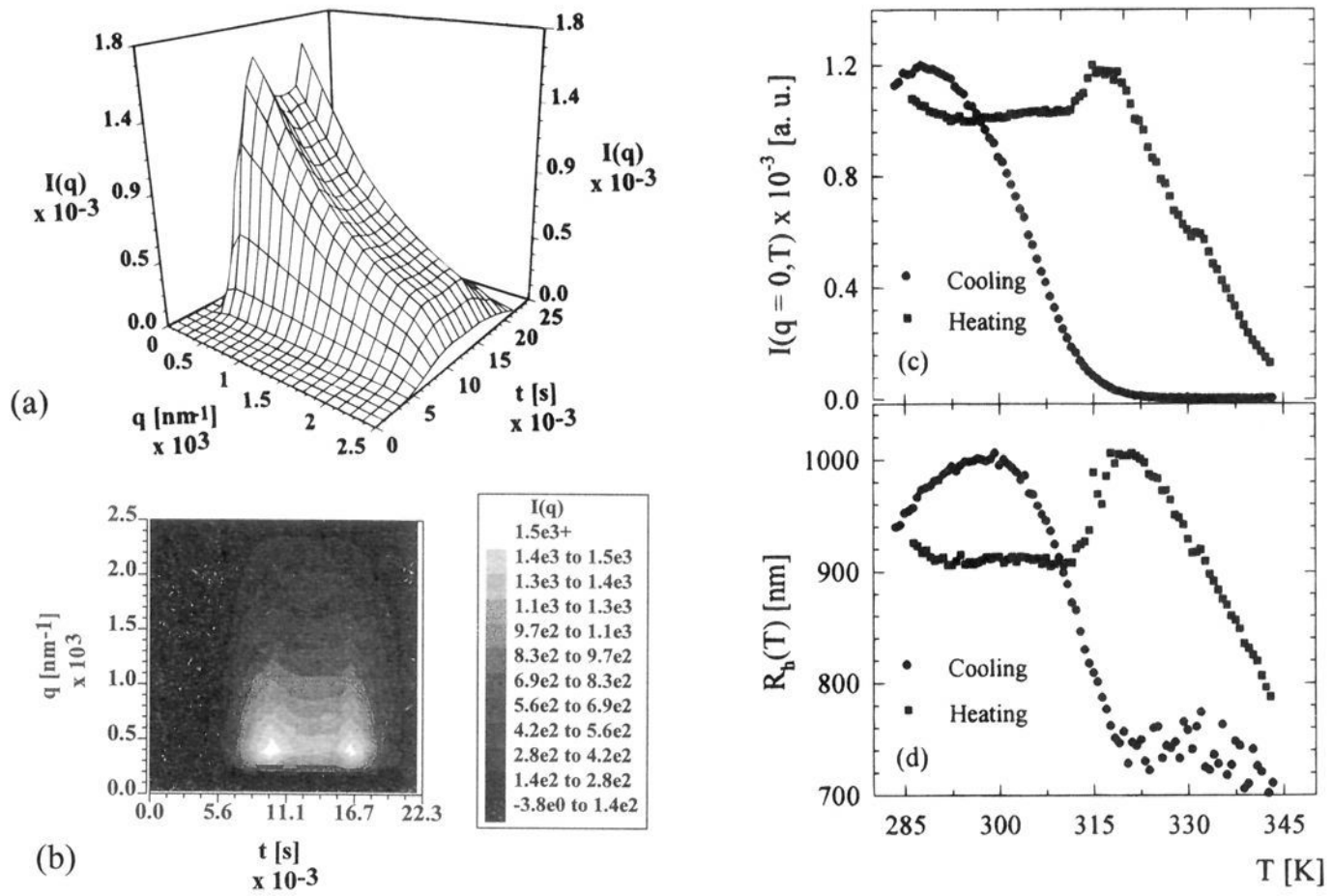

Figure 7. (a) Surface and (b) spectral plot of the cooling−heating transition of β-CD followed by small-angle SLS. In order to ease data handling, 720 images are averaged in sets of 10. The gradient step corresponds to 0.33 K/min. (c) Zero-angle-extrapolated intensity and (d) radius of gyration, as a function of temperature, from the same experiment. For clarity, in c and d, only every fourth point is displayed. The difference in free energy of crystal formation and dissolution is −30 kJ/mol.

can be attributed to the development of interfacial layers around the clusters.[15]

Hysteresis between Cooling and Heating Cycles. The small-angle SLS experiments are directed against observations of crystallites larger than those studied by DLS. Due to the smaller scattering vectors employed with this technique, minor populations of clusters that escape observation in the DLS experiment can be captured.

In Figure 7 we display a typical crystallization experiment involving a cooling−heating cycle of 45 mg/mL β-CD in water. The cooling and heating rates were identical, 0.33 K/min, albeit different than those employed in the DLS experiment. Therefore, direct comparisons are not meaningful at this stage.

Relevant parameters obtained from these experiments are (a) the radius of the evolving clusters and (b) the zero-scattering vector-extrapolated intensity that is considered to be proportional to the molecular weight of the clusters. The latter parameters are obtained from simple linear least squares-fits on the data according to the standard Guinier scheme.[29] This approach can be employed for compact structures. If this is not the case, *i.e.*, the clusters are fractals, a Fisher−Burford[30,31] fit on the data is necessary. Since in the present case plots of ln $I(\mathbf{q})$ vs $\mathbf{q}^2$ were linear, we can exclude the latter case.

The scattered intensity, cluster size, and molecular weight follow again sigmoidal kinetics, and the heating cycle of the crystallization transition exhibits a considerable hysteresis, Figure 7. The sizes span, in these experiments, the range between 700 nm and *ca.* 1 μm. The downward curvature observed in the cooling cycle below room temperature is attributed to sedimentation of the clusters. The leveling off and the observed peaks during the heating cycle are associated with a gradual dissolution and size decrement of the examined crystallites.

Despite sedimentation and neglecting a temperature dependent turbidity correction[32] of 11% determined by measuring transmission in a parallel experiment, one can still employ size and intensity estimates for obtaining tentative values of the free energies of the crystallite formation−dissolution process. Using again a two-state model and exploiting only the linear regions of both observables, we determine $\Delta G_c = -200$ kJ/mol and $\Delta G_h = -170$ kJ/mol, for the cooling and heating cycles, respectively. This leads to a free energy difference of −30 kJ/mol between the cooling and heating cycles. The latter could be understood as the excess energy required to break stable bonds of well-formed crystallites. It is however doubtful if the excess energy can directly be associated with "crystal forces", due to sedimentation effects. The observed hysteresis varies strongly with the initial β-CD concentration and the cooling or heating rate. Systematic studies on the behavior of these larger crystallites will be the subject of a subsequent communication.

Light Microscopy. Light microscopy studies indicate that the β-CD crystallites are thin parallelepipeds with an approximate axial ratio of 1:2 when their size reaches a few micrometers, Figure 8a−f. These crystallites sediment when the solution temperature is lowered close to room temperature. However, the samples contain narrowly peaked clusters with sizes below 1 μm that can be recognized early in the images.

In Figure 8a−f we display a preliminary analysis of the crystallite size during a cooling−heating cycle under conditions similar to those of the small-angle SLS. Due to the large amounts of crystallites that appear in the images as a function of temperature, we have employed a more dilute β-CD concentration of 30 mg/mL. For larger crystallite populations, the computer time required per image is prohibitively long. The mean area and compactness of visible crystallites when plotted as a function of temperature for each cycle exhibit again the sigmoidal tendency, for both area and compactness.

(29) Glatter, O. In *Neutron, X-Ray and Light Scattering*; Lindner, P., Zemb, Th., Eds.; North Holland: Amsterdam, The Netherlands, 1991.
(30) Fisher, M. E.; Burford, R. J. *Phys. Rev. A* **1967**, *156* (2), 583.
(31) Carpineti, M.; Ferri, F.; Giglio, M.; Paganini, E.; Perini, U. *Phys. Rev. A* **1990**, *42* (12), 7347.
(32) Rouw, P. R.; Woutersen, A. T. J. M.; Ackerson, B. J.; de Kruif, C. G. *Physica A* **1989**, *156*, 876.

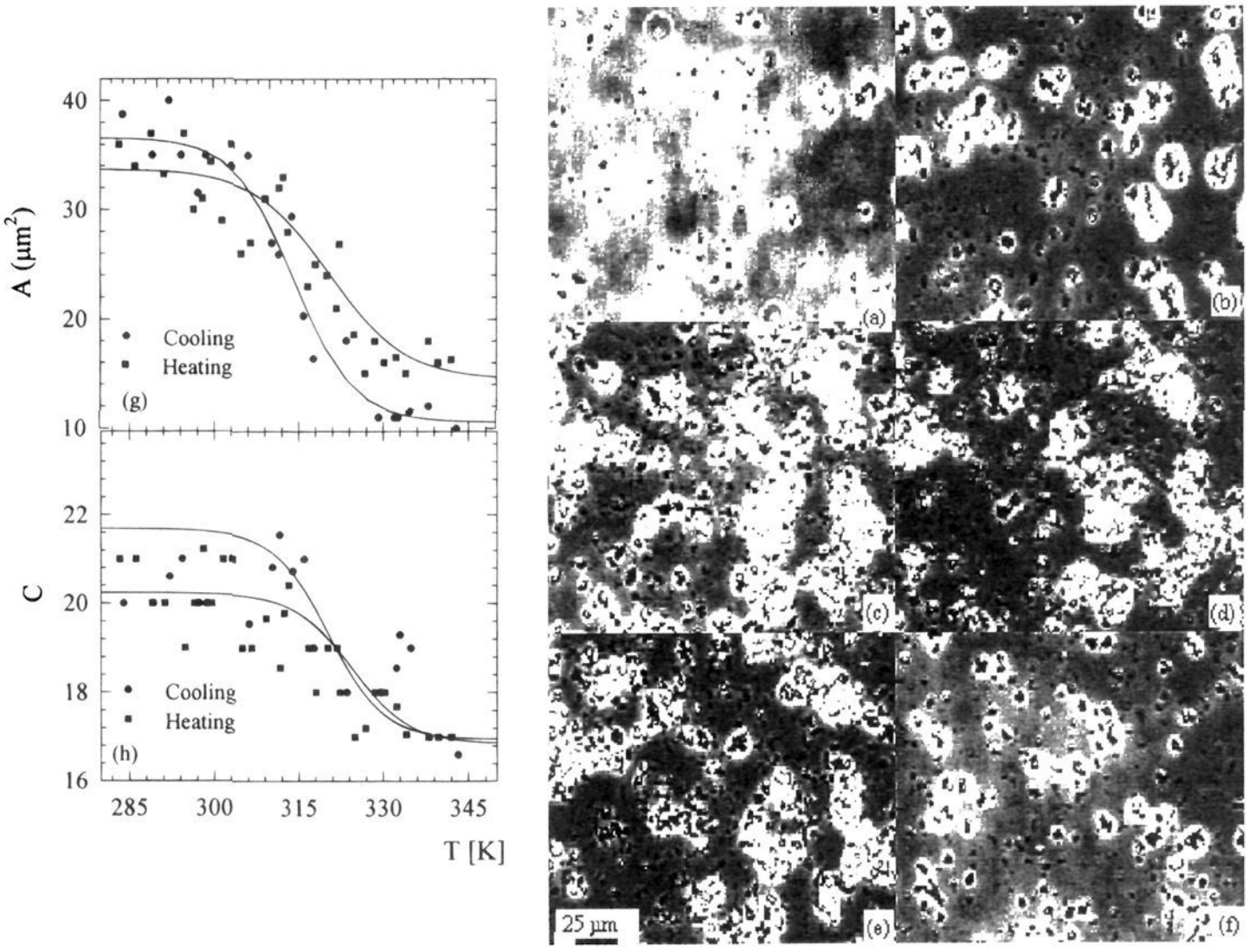

Figure 8. Typical digitized images of β-CD at (a) 343.2, (b) 308, and (c) 288.2 K during the cooling cycle and (d) 288.2, (e) 308, and (f) 343.2 K during the heating cycle. The original images have been subjected to a rescaling of gray values in order to increase contrast. Note the differences in the number of crystallites below and above T_c. (g) Average area, A, and (h) compactness, C, of the crystallites deduced from the same experiment. (The compactness, C, of an object is defined as $C = S^2/(4\pi A)$, where S denotes circumference and A is area of the object.) The series involved 265 temperature-resolved images, and analyses on every fifth image are displayed. A maximum number of only 70 objects has been randomly captured and examined in each image. Again, both observables obey sigmoidal kinetics; however, due to the mentioned limitations, the displayed curves serve only as guides to the eye.

Problems Associated with These Studies. Light scattering suffers from the presence of dust particles. Filtration is therefore an unavoidable constraint. During these experiments, filtration was found to be a very critical factor. The kinetics change drastically when standard filters, 100 nm pore radius, are employed because the initial cluster diameter comes close to the filter pore dimensions. Therefore, most of the subcritical nuclei will not penetrate the filters. These problems can be avoided by using larger, *e.g.*, 400 nm, pore radius filters. This size is larger than the radius of the largest clusters. The latter were determined to be, for unfiltered β-CD solutions, equal to 100−150 nm at 343.2 K. Another point that should not be disregarded is the mechanical strength of the evolving clusters. Forcing nucleating solutions through narrow pores may cause restructuring with unpredictable consequences on the kinetic process.

Reliable size estimates cannot be obtained unless solutions are transparent. Multiple scattering with concomitant signal decorrelation may be a potential obstacle when nucleating β-CD solutions cross-over T_c. This fact poses limits at the supersaturation range that can be safety explored. Probable alternatives to this problem may be cross-correlation techniques[33,34] or diffusion wave spectroscopy.[35]

Growth of large nuclei or microcrystals on the walls of the light-scattering vials is a major problem with β-CD solutions that often renders measurements impossible. This inconvenience may be only partially alleviated by using silanized light-scattering cells or by periodically rotating and translating the light-scattering cells. Additional problems arise from the sedimentation of crystallites through the scattering volumes when room temperature is approached.

The equilibrium shape of a cluster is approximated as a smooth sphere. This is certainly not correct, but there is no reason to complicate the issue by assuming other shapes, like cubes or polyhedra. In such a case, geometrical form factors have to be implemented in eqs 4−6 in order to account for deviations in the shape of the resulting nuclei from spherical.[36] As an example, if one assumes cubes instead of spheres for the equilibrium shape, n_c is expected to increase by a factor of 2.

Finally, the observation of at least two distinct populations through DLS and small-angle SLS indicates that the cluster distribution function is more complex than one could claim solely on the basis of the DLS experiments. A full reconstruction of the distribution will require temperature-resolved simultaneous multiangle SLS and DLS measurements, which is at present very difficult to technically access.

Conclusions

We have investigated the thermally induced crystallization of β-CD in water. DLS and SLS measurements can deliver pertinent information concerning the initial cluster formation. Both types of measurements are necessary to determine size, shape, and roughness of the evolving clusters. The obtained

(33) Schätzel, K. *J. Mod. Opt.* **1991**, *38*, 1849.
(34) Drewel, M.; Ahrens, J.; Podschus, U. *J. Opt. Am. Soc.* **1990**, *A7* (2), 206.
(35) Weitz, D. W. In *Dynamic Light Scattering, the Method and Some Applications*; Brown, W., Ed.; Oxford Science Publications: Oxford, U.K., 1993.
(36) Lieser, K. H. *Angew. Chem.* **1969**, *81* (6), 206.

results converge reasonably well to predictions dictated by the classical nucleation theory. We reckon that the observed transition resembles the transition from subcritical to postcritical nucleation.

An aspect for which we do not yet have satisfactory explanations concerns the initial size of β-CD clusters and consequently the number of monomers involved in the formation of a nucleus. One would expect to observe a gradual increment of the cluster size starting from only a few nanometers and progressively increasing to an initial size of 150 nm. Either the smaller sizes may be present at high temperatures, which we cannot investigate with our apparatus, or the nucleation burst is extremely rapid and cluster formation is immediate. The latter explanation seems to suit better the experimental findings; however, high-temperature experiments should be undertaken. Very recently, some interesting observations were made by X-ray scattering on zeolites.[37] These experiments indicate that nucleation, in contrast to classical theories, occurs via formation of small fractal structures. These clusters undergo restructuring, and after rearrangements in solution, a dense microcrystalline phase is formed. Whereas it would be rather premature to extend such mechanisms to cyclodextrins, these observations render indirect support to our findings.

The sigmoidal character of the kinetics of cluster formation allows us to access growth rates and obtain estimates of the free energy. We have also to note that the observed transition is not that steep as the transition measured in earlier studies[7] through turbidity. This may be due to either faster cooling rates employed or vigorous stirring, whereas the solutions in our experiments were kept undisturbed. Estimates of the free energy accompanying the transition can be obtained assuming a simple two-state model, whereas a considerable hysteresis is observed between the cooling and heating cycles.

The evolving clusters appear to be compact in contrast to protein precrystallization clusters where significant amounts of tenuous, mass fractal aggregates, with fractal dimension $d_f \approx 1.8$, dominate the scattering process.[38-41] The behavior indicates that β-CD monomers pack very efficiently, probably because the O2, O3, and O6 hydroxyl groups can replace water of hydration when molecules interact. In contrast, protein molecules are loosely packed due to their complex shape, charged side chains, and tighter hydration sphere. Subcritical clusters appear more compact than postcritical ones. Theoretical studies[42,44] indicate that deviations from the classical nucleation picture are quite probable. When small compact clusters evolve in time, the probability of collision increases. Such clusters will then fail to interpenetrate each other as they did when they were small. Therefore, the growth of less compact structures at lower temperatures is not unexpected.

Finally, the mechanism of growth can be classified, below T_c, as coalescence.[45] This is shown in Figure 9 where the

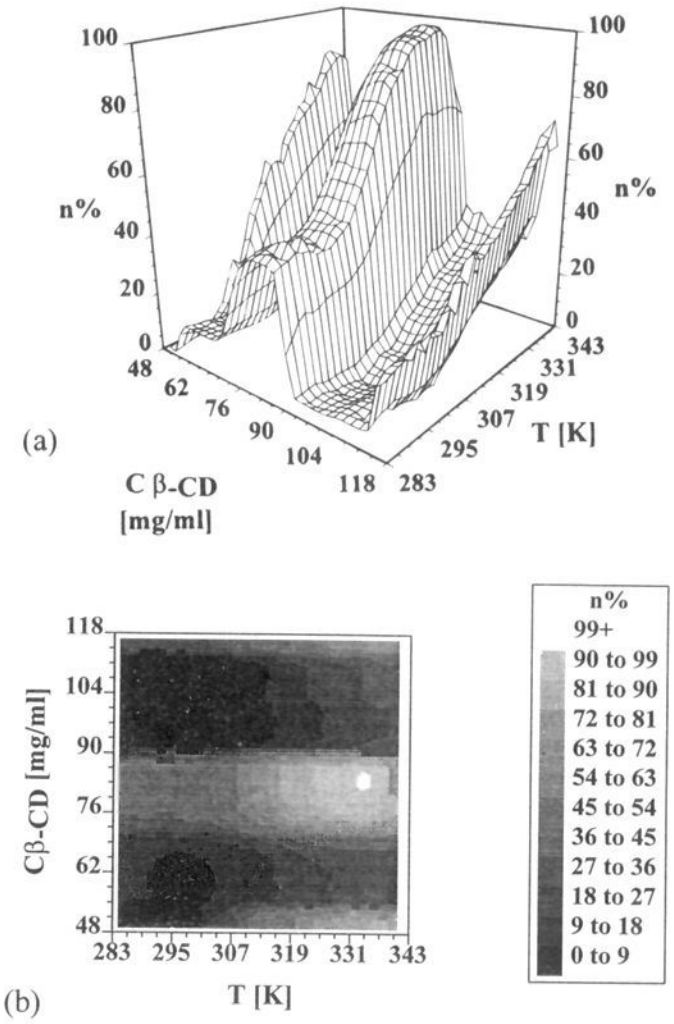

Figure 9. (a) Surface and (b) spectral plot of the relative change on the number of nuclei plotted as a function of temperature and β-CD concentration. The relative number appears to drop in a sigmoidal fashion with a minimum centered around 307.2 K and 83.3 mg/mL β-CD. The number of nuclei remains nearly constant below T_c.

percentage of nuclei, eq 11, is plotted as a function of β-CD concentration and temperature. A substantial drop of the relative amount of nuclei, as temperature approaches T_c and *ca.* 83.0 mg/mL, is observed. The expected development of the scattering profiles is compatible with the evolution of large domains growing at the expense of small ones (compare with Figure 2).

CDs due to their simple crystallization conditions can provide important insights in the issues of nucleation and crystal growth. They also exhibit the advantage that they are uncharged in contrast to proteins. Therefore, only hydrogen bonding and van der Waals interactions should be considered if theoretical computations for nuclei formation are undertaken.

Considering the assumptions and pitfalls involved in the classical nucleation theory from the melt, as well as the technical problems encountered, the essential physics of thermally induced nucleation in nonhomogeneous binary solution can be captured with adequate precision. Further research on the controlled crystallization of cyclodextrin inclusion compounds is under way.

Acknowledgment. Financial support to Y.G. by the European Space Agency (ESA/ESTEC) the Deutsche Forschungsgemeinschaft (Sa. 196/26-1), and the Fonds der Chemischen Industrie is deeply acknowledged. We also thank Drs. M. D. Soumpasis, P. Zielenkiewicz, and T. Steiner for several illuminating discussions and Mr. J. Frank for conducting the DSC experiments.

JA950805K

(37) Dokter, W. H.; van Garderen, H. F.; Beelen, T. P. M.; van Santen, R. A.; Bras, W. *Angew. Chem.* **1995**, *107* (1), 122.
(38) Georgalis, Y.; Zouni, A.; Eberstein, W.; Saenger, W. *J. Crystal Growth* **1993**, *126*, 245.
(39) Georgalis, Y.; Saenger, W. *Adv. Colloid Interface Sci.* **1993**, *46*, 165.
(40) Georgalis, Y.; Schüler, J.; Eberstein, W.; Saenger, W. In *Fractals in the Natural and Applied Sciences*; Novak, M. M., Ed.; Elsevier Science B. V.; North-Holland: Amsterdam, The Netherlands, 1994; p 139.
(41) Eberstein, W.; Georgalis, Y.; Saenger, W. *J. Crystal Growth* **1994**, *143*, 71.
(42) Klein, W.; Leyvraz, F. *Phys. Rev. Lett.* **1986**, *57* (22), 2845.
(43) Heermann, D. W.; Klein, W. *Phys. Rev. Lett.* **1982**, *50* (14), 1062.
(44) Yang, J.; Gould, H.; Mountain, R. D. *J. Chem. Phys.* **1990**, *93* (1), 711.
(45) Gunton, J. D.; San Miguel, M.; Sahni, P. S. In *Phase Transitions and Critical Phenomena 8*; Domb, C., Lebowitz, J. L., Eds.; Academic Press: New York, 1988; p 267.